Computers and Electronics in Agriculture 172 (2020) 105342

Contents lists available at ScienceDirect

Computers and Electronics in Agriculture

journal homepage: www.elsevier.com/locate/compag

SoyNet: Soybean leaf diseases classification

Aditya Karlekar[a], Ayan Seal[b,*]

[a] Hitkarini College of Engineering and Technology, Jabalpur 482005, India
[b] PDPM Indian Institute of Information Technology, Design and Manufacturing, Jabalpur 482005, India

ARTICLE INFO

Keywords:
Soybean leaf diseases identification
Background separation
Convolution neural networks

ABSTRACT

According to studies, the human population would cross 9 billion by 2050 and the food demand would increase by 60%. Therefore, increasing and improving the quality of the crop yield is a major field of interest. Recently, infectious biotic and abiotic diseases reduce the potential yield by an average of 40% with many farmers in the developing world experiencing yield losses as high as 100%. Farmers worldwide deal with the issue of plant diseases diagnosis and their proper treatment. With advancements of technology in precision agriculture, there has been quite a few works done for plant diseases classification although, the performances of the existing approaches are not satisfactory. Moreover, most of the previous works fail to accurately segment leaf part from the whole image especially when an image has complex background. Thus, a computer vision approach is proposed in order to address these challenges. The proposed approach consists of two modules. The first module extracts leaf part from whole image by subtracting complex background. The second module introduces a deep learning convolution neural network (CNN), SoyNet, for soybean plant diseases recognition using segmented leaf images. All the experiments are done on "Image Database of Plant Disease Symptoms" having 16 categories. The proposed model achieves identification accuracy of 98.14% with good precision, recall and f1-score. The proposed method is also compared with three hand-crafted features based state-of-the-art methods and six popularly used deep learning CNN models namely, VGG19, GoogleLeNet, Dense121, XceptionNet, LeNet, and ResNet50. The obtained results depict that the proposed method outperforms nine state-of-the-art methods/models.

1. Introduction

Nowadays, soybean (*Glycine max L. Merrill*) is one of the most imperative seed legumes in the world. It is the principal source of edible oil and it contributes nearly 25% of the world's total edible oil (Agarwal et al., 2013). Nutritional value of soybean helps to prevent heart disease and diabetes to a certain extent. India is the fifth largest soybean producing country in the world after United States, Brazil, Argentina and China. Over the past few years, the average annual yield loss of the soybean crop reached nearly 11% in United States only due to diseases (Hartman et al., 2015). Inadequate plant protection procedures, increase in pathogen varieties and poor cultivation practices are some of the reasons of a shoot up in intensity of damage caused by diseases in soybean plants. This study focuses on classification of soybean plant diseases based on the natural warning patterns/signs of the diseases appearing on the leaves of the plant. Soybean leaf diseases have various symptoms. Generally, there are fifteen types of leaf diseases, including Anthracnose, Bacterial Blight, Soybean Mosaic Virus, Copper Phytotoxicity, Charcoal Rot, Leaf Cercospora, Rhizoctonia Aerial Blight, Downy Mildew, Southern Blight, Powdery Mildew, Powdery Mildew and Rust, Phytophora Rot, Rust, and Brown Spot (Barbedo and Godoy, 2015). In early days, farmers identified these diseases by visual inspection of symptoms appearing on the leaves. The process of manual identification is quite challenging for a novice or inexperienced farmer than for professional plant pathologists (Miller et al., 2009). Human intervention was needed to classify those diseases either by scrutinizing the physical appearance of plant i.e. characteristics of the visual symptoms, or by carrying out some laboratorial examination. The high-accuracy, early detection and diagnosis of plant diseases are essential in precision agriculture for reduction of losses in crop yield especially in soybean production both qualitatively and quantitatively (Huang et al., 2014). An automatic reliable computer-aided system is desired to assist farmers, which can detect and identify diseases by observing the appearance of a plant and visual symptoms. Thus, building technologies to precisely identify the proper soybean leaf diseases is essential for disease prevention. With the advent of artificial intelligence and computer vision technologies, few efforts were made for a quick and accurate classification of soybean leaf diseases caused by biotic and abiotic constraints (Zhang et al., 2018; Chouhan et al., 2018). However, it requires further study to distinguish several diseases. S. Shrivastava

* Corresponding author.
E-mail address: ayan@iiitdmj.ac.in (A. Seal).

https://doi.org/10.1016/j.compag.2020.105342
Received 29 November 2019; Received in revised form 3 March 2020; Accepted 8 March 2020
Available online 21 March 2020

et al. presented a digital image processing based approach to detect and classify only two types of diseases namely, brown spot and frog eye (Shrivastava and Hooda, 2014). A total 100 images having 1600 × 1200 pixels resolution was considered for their work. All the images were captured using Samsung mobile model GT-S3770 digital camera. Morphological operation followed by thresholding was applied on input images in order to extract leaf part from the whole image and then identification of the infected region was carried out. Shape features of infected region were fed into K-Nearest Neighbor (KNN) classifier for identification of the above said diseases. The recognition rates are 70% and 80% for brown spot and frog eye respectively. The limitations of the above method are as follows: only two types of diseases were considered for their study, further their recognition rates are not enough in present context. S. Shrivastava et al. presented another work on automatic soybean plant foliar disease severity detection and estimation (Shrivastava et al., 2015). For the prediction of diseases-level, three indexes namely, disease severity index, infection per region, and disease level parameter were considered. All the experiments were performed on six types of soybean plant diseases namely, rust, bacterial blight, sudden death syndrome, brown spot, downy mildew, and frog eye. Before finding out the values of these indexes, leaf part was extracted from cluttered scene. However, the used segmentation algorithm fails to extract the leaf part from the cluttered scene due to complex background. In Gui et al. (2015), J. Gui et al. discussed a salient region based approach for soybean leaf disease detection. Low-level luminance and color features with multi-scale analysis to determine saliency maps were fed into k-means to extract disease regions. However, J. Gui et al. did not mention how many different types of diseases were used for their experiments and classification rates. J. C. A. Barbedo et al. presented a color transformation based approach (Barbedo and Godoy, 2015). A total of 372 images containing symptoms of 9 different diseases namely, bacterial blight, rust, phytotoxicity, stem canker, corynespora leaf spot, myrothecium leaf blight, downy mildew, powdery mildew, and septoria brown spot were considered. All the RGB color images were initially transformed into HSV, Lab and CMYK color spaces for extracting the intensity histograms from the gray-scale representations of each resulting channel. It is observed from the confusion matrix that the average recognition rate is not convincing. In Pires et al. (2016), R. D. L. Pires et al. discussed a method to detect soybean diseases using image local descriptors and bag of visual words. Four classes namely, mildew, rust tan, rust RB, and healthy leaf were considered. A total 1200 scanned leaf images were considered for their experiments. Out of eight local descriptors, pyramid histograms of visual words provided the best result i.e. 98% accuracy. An image retrieval based detection and identification method was discussed in Shrivastava et al. (2017) for five soybean leaf diseases namely, bacterial blight, brown spot, frog eye, rust and sudden death syndrome. Color histogram and wavelet decomposed color histogram along with border/interior classification, color coherence vector, color difference histogram, square symmetric local binary pattern, localized angular phase, and structure element histogram were exploited as feature extraction techniques. Various distances measures such as L1 distance, Euclidean distance, Canberra distance, Cosine distance, Chi-square distance, and D1 distance were used to find similarity score between the descriptor of query image and database images in order for image retrieval. After feature extraction, support vector machine (SVM), KNN and probabilistic neural network (PNN) were chosen for classifying leaf diseases. The highest accuracy is 93.3% and it was achieved using gray-level co-occurrence matrix texture features along with PNN. The achieved results are satisfactory however, there is a chance of improvement of the overall accuracy of the soybean leaf diseases detection and classification system. In Liang et al. (2018), W. Liang et al. presented an estimation method for soybean leaf area, edge, and defoliation using color image analysis. However, W. Liang et al. did not consider leaf diseases classification in their work. S. Kaur et al. used a rule based semi-automatic system using k-means to differentiate healthy leaf images from diseased leaf images (Kaur et al., 2018). Moreover, a diseased leaf was further classified into one of the three categories namely, downy mildew, frog eye, and septoria leaf blight. Research was accomplished on PlantVillage dataset by separately exploiting color features, texture features, and their combinations to train three models using SVM. The maximum average accuracy is about 90%, which cannot meet the current requirements for high recognition accuracy.

Therefore, in the follow-up study, we should focus on how to improve the identification accuracy. Over the past few years, convolutional neural networks (CNN) has made incredible improvements (LeCun et al., 2015; Guo et al., 2016). Nowadays, it can extract suitable feature portrayal from a large number of input images. It is an opportunity for plant pathologists or farmers to classify soybean leaf diseases in a judicious manner using deep learning, which helps to enhance the accuracy of plant protection and also extend the capacity of computer vision in the area of precision agriculture. Even though a number of deep neural networks exists for image classification task, most of them do not pan well when faced trained on data that requires a thorough understanding of the inherent features for classification. In this study, a computer aided diseases classification system is proposed, which consists of two modules namely, image processing module (IPM) and CNN module. The first module extracts the leaf region only from whole image by subtracting complex background. In second module, SoyNet is introduced to increase the classification accuracy of soybean leaf diseases in order to leverage the efficacy of a deep CNN for object classification. The proposed model is specifically built to learn the intricate features that are exhibited by different diseases in the soybean plant. All the experiments are performed on “Image Database of Plant Disease Symptoms (PDDB)” (Barbedo et al., 2016). The test results prove that our proposed model is successfully able to learn the less pronounced and more nuanced details about the infected leaf structure and is able to classify them correctly when tested on novel data.

The rest of this study is organized as follows. Section 2 deals with the materials used to perform the experiment in the form of database description, IPM and CNN. Experimental results are described and analyzed in Section 3. In Section 4, the proposed method is compared with some traditional methods and deep learning based approaches. Finally, this study is concluded in Section 5.

2. Material and method

In this section, the database used for validating the SoyNet along with state-of-the-art methods/models is presented followed by details of IPM and SoyNet.

2.1. Database

In this study, all the soybean leaf images are considered from publicly available benchmark database named as PDDB. It consists of a total of 486 RGB color soybean leaf images. Each image includes only one disease with complex background. There are 3 categories mainly called as healthy, infected and unknown. Infected leaves can be divided into 14 sub-categories, which are Anthracnose, Bacterial blight, Carijo Leaf, Charcoal Rot, Copper Phytotoxicity, Leaf Cercospora, Mela/Rhizoctonia aerial blight, Mildio/Downy mildew, Murcha Sclerocio, Oidio/Powdery mildew, Phytophora rot, Rust, Septoria/Brown Spot, Southern blight. All the images are not in same size. In other words, the number of pixels are not equal in all the images. Some sample images along with their diseases’ name are shown in Fig. 1.

2.2. Image augmentation

Training deep learning CNN requires substantial amount of images to reduce over-fitting and under-fitting. As the original dataset does not include enough images for proper training, it is necessary to expand the image set by applying various image augmentation techniques. The

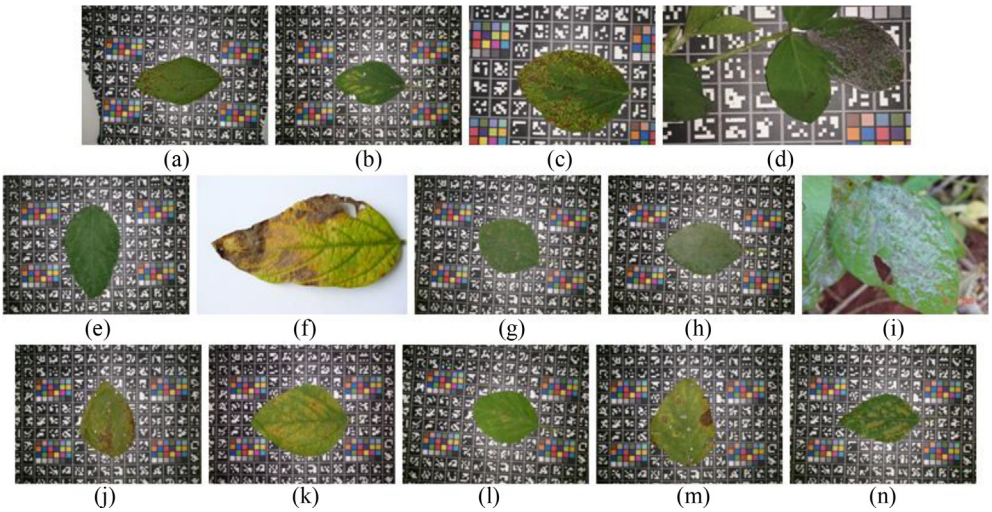

Fig. 1. Few sample leaf images of PDDB database: (a) Bacterial blight, (b) Soybean Mosaic Virus, (c) Copper Phytotoxicity, (d) Charcoal Rot, (e) Healthy, (f) Leaf Cercospora, (g) Downy mildew, (h) Powdery mildew, (i) Powdery mildew and Rust, (j) Rust, (k) Rust and target spot. (l) Brown spot, (m) Southern blight, and (n) Unknown.

Table 1
Statistics of augmented image set.

Name of the disease	Number of training images	Number of testing images
Anthracnose (P_1)	642	296
Bacterial blight (P_2)	701	305
Carijo Leaf (P_3)	704	286
Charcoal Rot (P_4)	720	300
Copper Phytotoxicity (P_5)	1136	470
Healthy (P_6)	646	281
Leaf Cercospora (P_7)	626	279
Mela (P_8)	560	270
Mildio (P_9)	685	284
Murcha Sclerocio (P_{10})	633	283
Oidio (P_{11})	719	282
Phytophora rot (P_{12})	1019	424
Rust (P_{13})	874	375
Septoria (P_{14})	794	361
Southern blight (P_{15})	801	377
Unknown (P_{16})	808	299
Total (P_{17})	12068	5172

augmented image set is created by rotating, translating and scaling, flipping the images vertically and horizontally, and applying random zooming. Moreover, an augmented image set is created by adding noise (Fawzi et al., 2016), color jittering (Krizhevsky et al., 2012), PCA jittering (Krizhevsky et al., 2012), rotation blur (Lin et al., 2018), and scaling blur (Dellana and Roy, 2016). Equal parity for individual class is ensured during augmentation. The augmented image set consists of 17,240 images out of which 12,068 (70%) are used for training and 5172 (30%) are used for testing. The statistics of image set after augmentation is reported in Table 1.

2.3. Image processing module

It is observed that the area of leaf part is comparatively smaller than the area of background in almost all the images of PDDB database. The area of infected regions in a leaf are very small as compared to background as well. So, if we train CNN without background subtraction then the classification accuracy may be decreased. In other words, if the leaf part is segmented from the whole image prior to training then CNN can easily find and learn relevant features to diseases detection/classification even when the number of images is limited. So, it is especially important to do background subtraction as the infected areas are small before training because smaller infected areas the harder for a CNN to pick them up. Therefore, IPM is required to remove background from the whole image. IPM consists of four sub-modules and their outputs are shown in Fig. 2.

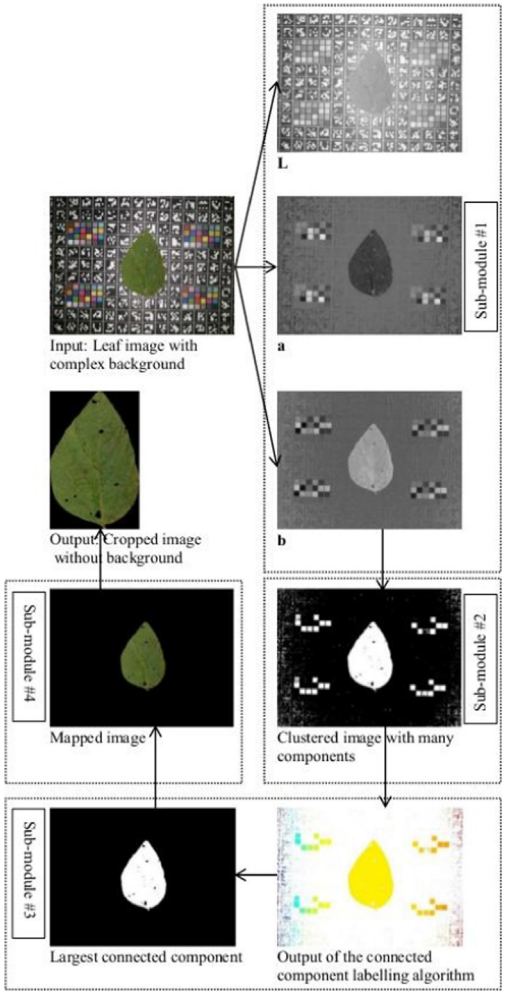

Fig. 2. Image processing module for background subtraction.

The first sub-module converts a RGB color leaf image to CIELab color space (Panigrahy et al., 2019). Here, Lab color space is explored because it closely matches with human perception. Unlike RGB color model, it is widely employed in image clustering (Achanta et al., 2012). Mathematically, Lab color space is a three-dimensional real number

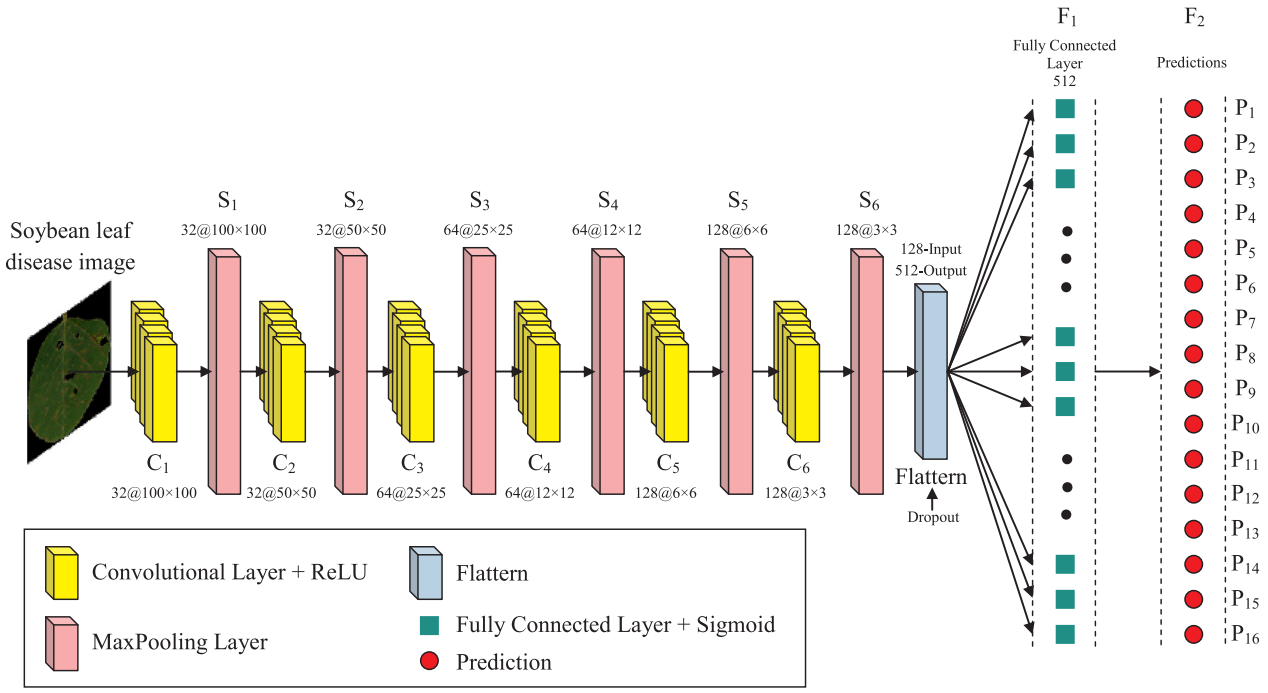

Fig. 3. Schematic block diagram of SoyNet.

space, where **L**, **a**, and **b** represent lightness, green/red color, and blue/yellow color respectively. The output of b-channel i.e. **b** feeds into the sub-module #2 as input.

The second module consists of traditional k-means clustering (Schellekens and Jacques, 2018; Chakraborty and Das, 2017; Maulik and Bandyopadhyay, 2002) as a tool. It identifies some inherent structure existing in **b** channel. The aim of k-means cluster analysis is to split **b** channel into ($k = 2$) foreground and background so that the pixels in the foreground are similar in some perception and pixels in the background in different clusters are dissimilar in the same perception. The output of the sub-module #2 is shown in Fig. 2. Here, white color i.e. logical 1 is used to represent foreground and background is illustrated by black color i.e. logical 0. In this experiment, two channels namely, **L** and **a** have not used as these two channels neither separately nor jointly give the good output. However, goodness is measured by visual inspection only. Then the output of the second sub-module feeds into the sub-module #3 as input.

The task of the third sub-module is to find out and extract the largest component because it is observed that the largest component illustrates the region of interest i.e. leaf part for this study. However, image consists of leaf part as well as other unwanted/irrelevant components. So, there is a need to remove unwanted components. For this purpose, connected component labelling algorithm (Seal et al., 2015; Morse, 2000) is exploited to get the number of components present in an image. All the connected components are marked by different colors, which are treated as the intermediary outputs of the sub-module #3 and are shown in Fig. 2. Then the largest component is extracted from all the connected components and say it as leaf part or region of interest. It means a binary image is obtained, where logical 1 represents the leaf part and the background is denoted by logical 0. Then this binary image acts as a mask in the sub-module #4 and maps it to the original RGB input image to get the RGB color leaf part only. In this way, complex background can be eliminated. However, the area of background is greater than the leaf part. So, leaf part needs to be cropped. A simple iterative algorithm starts working with the help of two pointers. The first pointer traverses from the top-left corner to the top-right corner of the output image of the sub-module #4 in order to find out the location of the first non-zero element from the top. On the other hand, the second pointer traverses from the bottom-left corner to the bottom-right corner so that the location of the first non-zero element can be obtained from the bottom. It means two pixel locations are identified, one from the top and other one from the bottom. These two pixel locations help to crop the output image from the top and the bottom and produce an intermediary image. Similarly, we can determine the left-most and the right-most non-zero elements and their pixel locations. These two pixel locations assist to crop the intermediary image from left-side and right-side of the intermediary image in order to generate cropped leaf image. This IPM is applied on all the images present in PDDB database in order to crop leaf part and remove irrelevant background. However, the IPM works fine in most of the cases. In few cases it extracts only the infected areas instead of giving leaf part. Total numbers of pixels are not same after cropping leaf part of all the images. So, the images are made consistent and reshaped to $100 \times 100 \times 3$ pixels using cubic bi-linear interpolation.

2.4. Convolutional neural networks module

Deep learning is a class of machine learning algorithms. A deep CNN can extract higher level features progressively from the input images by the multiple layers used in a model. Some of the most popularly used models are VGG19 (Simonyan and Zisserman, 2014), ResNet50 (He et al., 2016), GoogLeNet (Szegedy et al., 2015), Dense121 (Huang et al., 2017), LeNet (LeCun et al., 1998), and XceptionNet (Chollet, 2017) for classifying images. However, these models do not always perform well on all the datasets that are too specific in their nature. These networks can learn the general features of the image well enough which allow them to distinguish among variety of categories. However, they do not train well when the differences between images is not pronounced. In soybean leaf diseases classification, the distinction between the diseases in many cases is not pronounced and to properly identify the disease, the network must have knowledge of more nuanced features of the data. The proposed network, SoyNet, is specifically designed to classify diseases in soybean plant. It can learn the more intricate features of the dataset which allows it to correctly categorize diseases. It is designed in such a way so that each successive layer can learn more intricate features of the leaf data. With each layer we have decreased the size of the

spatial resolution of an image, so that more intricate features of the leaf can be captured. Given the specialized nature of the network, we have been able to create a deep neural network that is more succinct in terms of network size as compared to other available networks. This section describes the structure of SoyNet in detail, which comprising of Convolutional layer, Activation functions like Softmax and rectified linear unit (ReLU), Pooling layer, and Dropout. The detail configuration of each layer of SoyNet is presented in the following sub-sections.

2.4.1. Model architecture

The model is depicted pictorially in Fig. 3. The SoyNet mainly consists of six convolutional layers (C_1, C_2, C_3, C_4, C_5, and C_6), six MaxPooling layers (S_1, S_2, S_3, S_4, S_5, and S_6), and two fully connected layers (F_1 and F_2). The convolutional layers are mainly responsible for increasing the model's representational ability. Each convolution network has a 3×3 filter, while the MaxPool layer has 2×2 filters.

2.4.2. Convolution layers

Convolution can be described as an operation on two functions and forms the basis of CNNs. In CNNs, the feature map is convoluted by multiple inputs and the result is passed through an activation function. The convolution in CNNs can be written as

$$S_i = A(I * M_i), \tag{1}$$

where convolution operation, $*$, is performed on extracted leaf image, I, with the a kernel or mask, M_i, in the *ith* layer and the convoluted leaf image is passed through activation function, A(.). The SoyNet has 6 convolution layers each with a filter of 3×3 size. The first two convolution layers has 32 neurons on contrary 64 neurons are there in the next two convolution layers. Finally, 128 neurons are present in final two convolution layers.

2.4.3. Activation function

- **Rectified Linear Unit:** The unsaturated ReLU activation is employed in all convolution network layers as it provides better results than saturated activation functions like sigmoid and tanh in the training phase. If the input, x, is positive then ReLU produces x as an output, otherwise it generates 0. Mathematically, the ReLU function is defined as follows:

$$ReLU(x) = \begin{cases} 0 \text{ if } x < 0 \\ x \text{ otherwise} \end{cases} \tag{2}$$

  It is also known as ramp function. It takes S_i as input, which is obtained by Eq. (1).
- **Softmax:** The softmax activation is utilized in the last dense layer to calculate the probability of predicted classes. The class with the highest probability is chosen as output. The softmax function is given by:

$$S(y_i) = \frac{e^{y_i}}{\sum_{j=1}^{K} e^{y_j}}, \tag{3}$$

  where e^{y_i} and e^{y_j} denote the probability belonging to the i and j categories respectively; K denotes the number of categories and it is initialized to sixteen in this work. The softmax function calculates the prediction of each category, $S(y_i)$.

2.4.4. Pooling

The number of training parameters tends to increase rapidly with increase in the number of convolutional layers. To overcome this problem pooling layers are used. The pooling layer reduces the overall output of the convolutional layer, and thus, reduces the number of trainable parameters by utilizing the overall spatial characteristic of a region to represent the entire region. The network makes use of MaxPooling with a window size of 2×2. The max pooling operation represents the value of the whole 2×2 window with the maximum value present in the window.

2.4.5. Loss function

The Loss function measures the disparity between the predicated output and the desired output (label value). The network makes use of categorical cross-entropy for calculating loss, ϕ. The categorical cross-entropy function is given as:

$$\phi = -\frac{1}{K}\sum_{n=1}^{K} [y_n \log \hat{y}_n], \tag{4}$$

where y and $\hat{y}$ represent the actual and the expected outputs respectively.

2.4.6. Optimization and weight updation

The objective of network training is to find the value of W for which the loss value L minimizes. To ensure a faster training convergence, the model uses Adaptive Moment Estimation (Adam) for optimization and weight updation. The weights updation rules are as follows:

while W_t not converge,
$t \leftarrow t + 1$,
$g_t \leftarrow \nabla_W \phi(W_{t-1})$, where g_t is gradient at time t along W.
$m_t \leftarrow \beta_1 m_{t-1} + (1 - \beta_1) g_t$, where m_t is exponential average of gradient along W.
$v_t \leftarrow \beta_2 v_{t-1} + (1 - \beta_2) g_t^2$, where v_t is exponential average of squares of gradient along W.

m_t and v_t estimate the first and second moment of gradients respectively. As m_t and v_t are initialized as vectors of 0's, observed that they are biased towards zero, especially during the initial time steps, and especially when the decay rates are small (i.e. β_1, β_2 are close to 1). Perevented above problem by computing bias-corrected first and second moment estimates.

$\widehat{m_t} \leftarrow \frac{m_t}{(1-\beta_1^t)}$,
$\widehat{v_t} \leftarrow \frac{v_t}{(1-\beta_2^t)}$,
Then we can use the following expressions to update the parameters:
$\nabla_{W_t} \leftarrow \nabla_{W_{t-1}} - \frac{\alpha \widehat{m_t}}{(\sqrt{\widehat{v_t}} + \epsilon)} \cdot g_t$, where α is the learning rate, and β_1 and β_2 are the hyper parameters such that $\beta_1, \beta_2 \in [0, 1)$.
Then we add updated weight to out network for further process.
$W_{t+1} \leftarrow W_t + \nabla_{W_t}$

2.4.7. Dropout

Dropout refers to shutting off units (both hidden and visible) in a neural network. As the network continues to train, features that have better representation in the data dominates the learning process and the weights associated with these features get stronger. The dropout alleviates this situation by deliberately shutting down dominant neurons along with weights associated with them and helps the network learn underrepresented features. To prevent over fitting and improve generalization, a dropout was added to the network.

2.4.8. Hyper parameters

The model's hyper parameters are tabulated in Table 2. The model uses Adam as the solver type. The base learning rate is set to 0.001. The batch training is used to divide the training and testing sets into multiple batches. Each batch consists of 64 images.

3. Experimental results and discussion

3.1. Equipment

The Keras framework, Anaconda Development Environment and

Table 2
Hyper parameters used for training.

Name	Parameter
Solver type	Adam
Learning rate	0.001
β_1	0.9
β_2	0.999
Batch Size	64

Table 3
Configurations of Machine.

Name	Parameter
Memory	12.6 GB
Processor	Xeon Processor @2.3 GHz
Graphics	1xTesla K80
Language	Python

Python language are used to train and test the model. The basic configuration is shown in Table 3. The SoyNet is implemented for leaf diseases classification and therefore, it is decided to directly train the network from the scratch. This training strategy contributes to making the SoyNet significantly different from the other networks used in this study.

3.2. Evaluation metric

One of the widely used evaluation metrics is accuracy. It refers to how close a predicted value generated by a machine algorithm to its actual value. The higher value of accuracy corresponds to better performance. However, the use of accuracy alone can be misleading because of the accuracy paradox. So, accuracy is used with other performance metrics namely, precision, recall, and f1-score (Hossin and Sulaiman, 2015; Silva et al., 2019; Sharma and Seal, 2019) to evaluate machine learning algorithms. All the above said metrics depend on confusion matrix. Here, these metrics are used to compare the proposed method with state-of-the-art methods.

3.3. Model training

As it is not prudent to utilize all the available data for training purpose, the dataset is divided into training and validation sets. Seventy percentage of the augmented images in each category are randomly selected for training while remaining 30% constituted as validation set.

3.4. Results and discussion

Fig. 4 illustrates the decrease in training and test sets loss with successive iteration. As the model learns, it successfully reduces the loss value and showcases a proper convergence towards the global minima. The training and test loss reach their minimum values at around $40th$ epoch after which the loss values have remained relatively unchanged. Fig. 5 showcases the increase in accuracy of training and test sets with successive iteration. Table 4 shows the minimum loss and maximum accuracy achieved for training and test sets.

Table 5 records the precision, recall and f1 score along with their macro, micro and weighted averages for all categories in the test set with Fig. 6 showing the graphical representation of it. It can be noted that Phytophora rot has achieved the highest values in all three measures. This can be attributed to the distinctive brown coating covering the leaf. The lowest accuracy was achieved by Septoria while the lowest recall was for Bacterial blight. Bacterial blight has a high commonality with other diseases such as rust while the spot that appears on leaves infected by Septoria are so small that the leaves could easily be

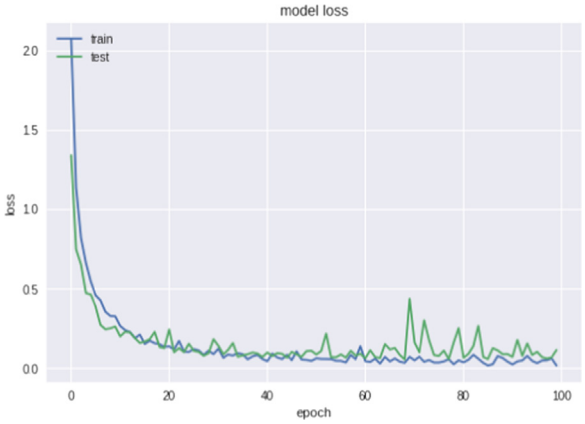

Fig. 4. Illustrating loss value per epoch for training and test sets.

Fig. 5. Illustrating accuracy per epoch for training and test sets.

Table 4
Illustrating Loss and Accuracy for training and test sets.

	Loss	Accuracy
Training	0.171	0.9945
Test	0.114	0.9814

Table 5
Tabulated precision, recall and f1-score values for test set.

	precision	recall	f1-score	support
P_1	0.99	1.00	0.99	296
P_2	0.98	0.84	0.90	305
P_3	0.99	0.99	0.99	286
P_4	1.00	1.00	1.00	300
P_5	0.99	0.96	0.97	470
P_6	0.96	0.99	0.98	281
P_7	0.99	1.00	1.00	279
P_8	1.00	1.00	1.00	270
P_9	0.99	0.99	0.99	284
P_{10}	1.00	1.00	1.00	283
P_{11}	0.97	0.94	0.96	282
P_{12}	1.00	1.00	1.00	424
P_{13}	0.97	0.90	0.93	375
P_{14}	0.87	1.00	0.93	361
P_{15}	0.88	0.95	0.91	377
P_{16}	0.98	0.99	0.98	299
micro avg	0.97	0.97	0.97	5172
macro avg	0.97	0.97	0.97	5172
weighted avg	0.97	0.97	0.97	5172

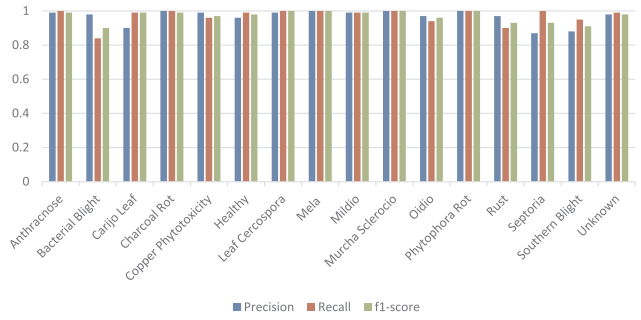

Fig. 6. Chart illustrating precision, recall and f1-score for test set.

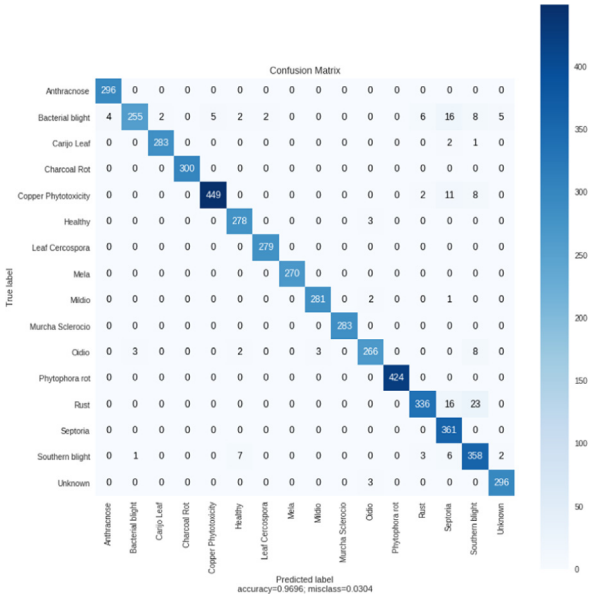

Fig. 7. Unnormalized confusion matrix.

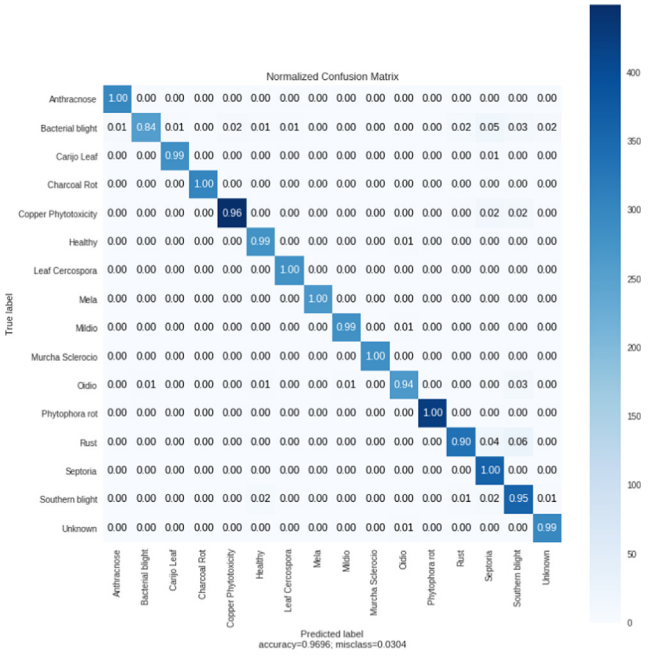

Fig. 8. Normalized confusion matrix.

misclassified as healthy. This explains the apparent low scores for these two categories.

Figs. 7 and 8 depict the confusion matrix comparing the true class against the predicted class. The calculated value describes the classification rate for individual classes. In the matrix higher color density signifies higher accuracy for the individual classes. Copper Phytotoxicity and Phytophora rot have the highest accuracy amongst the subclasses as can be noted by the color density in the confusion matrix. Fig. 9 depicts the output of every layer present in the model. The plot shows every channel in each of the 16 activation maps with channels stacked side by side. It should be noted that the first layer acts as a collection of various edge detectors. At this point, the activations retain almost all information present in the initial image. As we go deeper, the activations become increasingly abstract and less visually interpretable. The network begins to encode higher-level concepts such as leaf's spot and texture. These higher representations carry lesser information about the visual contents of the image, and increasingly more information regarding the class of the image. As the depth of the model increases, the sparsity of the activations increases too. In the first layer all filters are activated by the input image but in the following layers, more and more filters are blank. Thus, the deep neural network effectively acts as an information distillation pipeline which filters out irrelevant information from the input data (RGB image in this case) along with magnifying and refining the useful information.

4. Comparative study

All the state-of-the-art methods can be categorized into two groups. Methods in the first group are based on hand-crafted features only whereas CNN based models fall in the second group. In this work, SoyNet is compared with three hand-crafted features based methods and six popular CNN models namely, VGG19, GoogleLeNet, Dense121, XceptionNet, LeNet, and ResNet50. Hand-crafted features based methods are discussed in Section 1. However, the detail description of the above said CNN models are beyond the scope of this study. All the experiments are performed on PDDB database, which consists of 16 classes. The average accuracy, average precision, average recall and average f1-score obtained by all the above mentioned methods/models are reported in Table 6. It is clear from Table 6 that the SoyNet outperforms nine state-of-the-art methods/models.

5. Conclusion

In this work, mainly 3 types of soybean leaves called as healthy, infected and unknown are considered. There are 14 sub-types of infected leaves in PDDB database. So, altogether 16 categories are considered for this study. The proposed CNN, SoyNet, provides 98.14% accuracy with good precision, recall and f1-score when the train-test set is 70–30%. So, it depicts the effectiveness of the proposed method over three hand-crafted based state-of-the-art methods and six deep CNN models. This study illustrates that it is possible to achieve good accuracy by increasing the diversity of pooling operations, the reasonable addition of a Relu function and dropout operations, and including multiple adjustments of the model parameters. In future, other available soybean leaf diseases databases would be considered for training and testing SoyNet in order to check how it behaves.

Declaration of Competing Interest

The authors declare that they have no known competing financial interests or personal relationships that could have appeared to influence the work reported in this paper.

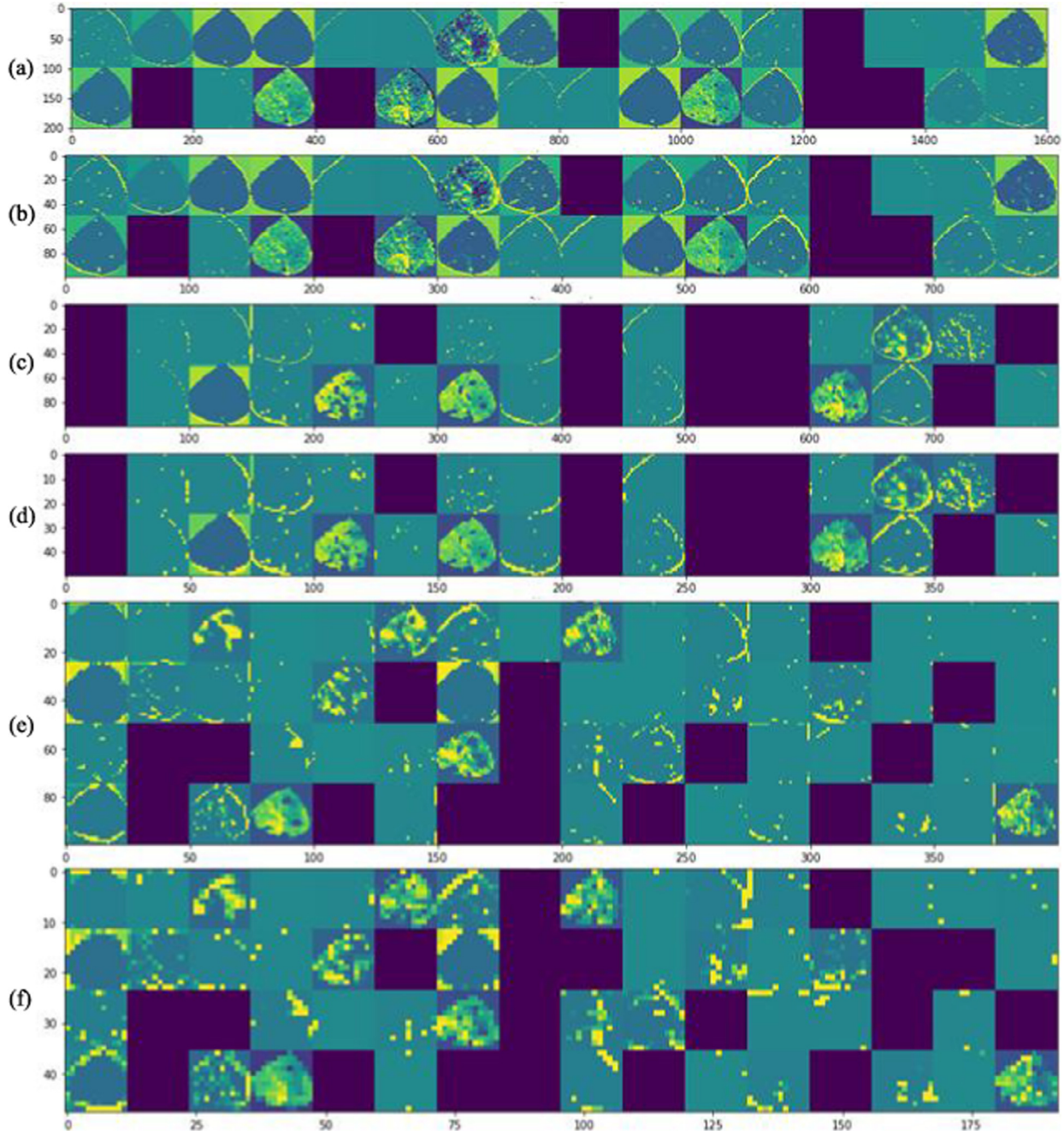

Fig. 9. Illustrating output of hidden network layers: (a) C_1, (b) S_1, (c) C_2, (d) S_2, (e) C_3, (f) S_3.

Table 6
Comparative evaluation of the proposed method with nine state-of-the-art methods.

Method	# training images	# testing images	Accuracy (%)	Precision (%)	Recall (%)	F1-score (%)
Shrivastava and Hooda (2014)	340	146	60.24	58	60.35	59.7
Shrivastava et al. (2015)	340	146	62.7	63	63	62.7
Kaur et al. (2018)	340	146	68.9	70	71	70.53
VGG19 Simonyan and Zisserman (2014)	12,068	5172	89	86	79	78
GoogleLeNet Szegedy et al. (2015)	12,068	5172	39	44	35	35
Dense121 Huang et al. (2017)	12,068	5172	98.14	54	48	49
XceptionNet Chollet (2017)	12,068	5172	59	74	54	52
LeNet LeCun et al. (1998)	12,068	5172	48	65	45	35
ResNet50 He et al. (2016)	12,068	5172	79	69	75	74
Proposed method	12,068	5172	**98.14**	**97**	**97**	**97**

Acknowledgment

This work is partially supported by the project “Prediction of diseases through computer assisted diagnosis system using images captured by minimally-invasive and non-invasive modalities”, Computer Science and Engineering, PDPM Indian Institute of Information Technology, Design and Manufacturing, Jabalpur India (under ID: SPARC-MHRD-231).

Appendix A. Supplementary material

Supplementary data associated with this article can be found, in the online version, at https://doi.org/10.1016/j.compag.2020.105342.

References

Achanta, R., Shaji, A., Smith, K., Lucchi, A., Fua, P., Süsstrunk, S., 2012. Slic superpixels compared to state-of-the-art superpixel methods. IEEE Trans. Pattern Anal. Mach. Intell. 34 (11), 2274–2282.

Agarwal, D.K., Billore, S., Sharma, A., Dupare, B., Srivastava, S., 2013. Soybean: introduction, improvement, and utilization in India—problems and prospects. Agric. Res. 2 (4), 293–300.

Barbedo, J.G.A., Godoy, C.V., 2015. Automatic classification of soybean diseases based on digital images of leaf symptoms. In: Embrapa Soja-Artigo em anais de congresso (ALICE), CONGRESSO BRASILEIRO DE AGROINFORMÁTICA, 10, 2015, Ponta Grossa. Uso de.

Barbedo, J.G.A., Koenigkan, L.V., Santos, T.T., 2016. Identifying multiple plant diseases using digital image processing. Biosyst. Eng. 147, 104–116.

Chakraborty, S., Das, S., 2017. k- means clustering with a new divergence-based distance metric: convergence and performance analysis. Pattern Recogn. Lett. 100, 67–73.

Chollet, F., 2017. Xception: deep learning with depthwise separable convolutions. In: Proceedings of the IEEE Conference on Computer Vision and Pattern Recognition, pp. 1251–1258.

Chouhan, S.S., Kaul, A., Singh, U.P., Jain, S., 2018. Bacterial foraging optimization based radial basis function neural network (brbfnn) for identification and classification of plant leaf diseases: an automatic approach towards plant pathology. IEEE Access 6, 8852–8863.

Dellana, R., Roy, K., 2016. Data augmentation in cnn-based periocular authentication. In: 2016 6th International Conference on Information Communication and Management (ICICM). IEEE, pp. 141–145.

Fawzi, A., Samulowitz, H., Turaga, D., Frossard, P., 2016. Adaptive data augmentation for image classification. In: 2016 IEEE International Conference on Image Processing (ICIP). IEEE, pp. 3688–3692.

Gui, J., Hao, L., Zhang, Q., Bao, X., 2015. A new method for soybean leaf disease detection based on modified salient regions. Int. J. Multimedia Ubiquitous Eng. 10 (6), 45–52.

Guo, Y., Liu, Y., Oerlemans, A., Lao, S., Wu, S., Lew, M.S., 2016. Deep learning for visual understanding: a review. Neurocomputing 187, 27–48.

Hartman, G.L., Rupe, J.C., Sikora, E.J., Domier, L.L., Davis, J.A., Steffey, K.L., 2015. Compendium of soybean diseases and pests. Am. Phytopath. Soc.

He, K., Zhang, X., Ren, S., Sun, J., 2016. Deep residual learning for image recognition. In: Proceedings of the IEEE Conference on Computer Vision and Pattern Recognition, pp. 770–778.

Hossin, M., Sulaiman, M., 2015. A review on evaluation metrics for data classification evaluations. Int. J. Data Min. Knowl. Manage. Process 5 (2), 1.

Huang, W., Guan, Q., Luo, J., Zhang, J., Zhao, J., Liang, D., Huang, L., Zhang, D., 2014. New optimized spectral indices for identifying and monitoring winter wheat diseases. IEEE J. Sel. Top. Appl. Earth Observ. Remote Sens. 7 (6), 2516–2524.

Huang, G., Liu, Z., Van Der Maaten, L., Weinberger, K.Q., 2017. Densely connected convolutional networks. In: Proceedings of the IEEE Conference on Computer Vision and Pattern Recognition, pp. 4700–4708.

Kaur, S., Pandey, S., Goel, S., 2018. Semi-automatic leaf disease detection and classification system for soybean culture. IET Image Proc. 12 (6), 1038–1048.

Krizhevsky, A., Sutskever, I., Hinton, G.E., 2012. Imagenet classification with deep convolutional neural networks. In: Advances in Neural Information Processing Systems, pp. 1097–1105.

LeCun, Y., Bottou, L., Bengio, Y., Haffner, P., 1998. Gradient-based learning applied to document recognition. Proc. IEEE 86 (11), 2278–2324.

LeCun, Y., Bengio, Y., Hinton, G., 2015. Deep learning. Nature 521 (7553), 436.

Liang, W.-Z., Kirk, K.R., Greene, J.K., 2018. Estimation of soybean leaf area, edge, and defoliation using color image analysis. Comput. Electron. Agric. 150, 41–51.

Lin, Z., Mu, S., Shi, A., Pang, C., Sun, X. et al., 2018. A novel method of maize leaf disease image identification based on a multichannel convolutional neural network.

Maulik, U., Bandyopadhyay, S., 2002. Performance evaluation of some clustering algorithms and validity indices. IEEE Trans. Pattern Anal. Mach. Intell. 24 (12), 1650–1654.

Miller, S.A., Beed, F.D., Harmon, C.L., 2009. Plant disease diagnostic capabilities and networks. Ann. Rev. Phytopathol. 47, 15–38.

Morse, S.B., 2000. Lecture 2: Image Processing Review, Neighbors, Connected Components, and Distance. Bringham Young University Copyright Bryan S. Morse.

Panigrahy, C., Seal, A., Mahato, N.K., 2019. Fractal dimension of synthesized and natural color images in lab space. Pattern Anal. Appl. 1–18.

Pires, R.D.L., Gonçalves, D.N., Oruê, J.P.M., Kanashiro, W.E.S., Rodrigues Jr, J.F., Machado, B.B., Gonçalves, W.N., 2016. Local descriptors for soybean disease recognition. Comput. Electron. Agric. 125, 48–55.

Schellekens, V., Jacques, L., 2018. Quantized compressive k-means. IEEE Signal Process. Lett. 25 (8), 1211–1215.

Seal, A., Bhattacharjee, D., Nasipuri, M., Basu, D.K., 2015. Ugc-ju face database and its benchmarking using linear regression classifier. Multimedia Tools Appl. 74 (9), 2913–2937.

Sharma, K.K., Seal, A., 2019. Modeling uncertain data using monte carlo integration method for clustering. Expert Syst. Appl. 137, 100–106.

Shrivastava, S., Hooda, D.S., 2014. Automatic brown spot and frog eye detection from the image captured in the field. Am. J. Intell. Syst. 4 (4), 131–134.

Shrivastava, S., Singh, S.K., Hooda, D.S., 2015. Color sensing and image processing-based automatic soybean plant foliar disease severity detection and estimation. Multimedia Tools Appl. 74 (24), 11467–11484.

Shrivastava, S., Singh, S.K., Hooda, D.S., 2017. Soybean plant foliar disease detection using image retrieval approaches. Multimedia Tools Appl. 76 (24), 26647–26674.

Silva, V.A., Bittencourt, I.I., Maldonado, J.C., 2019. Automatic question classifiers: a systematic review. IEEE Trans. Learn. Technol.

Simonyan, K., Zisserman, A., 2014. Very deep convolutional networks for large-scale image recognition. arXiv preprint arXiv: 1409.1556.

Szegedy, C., Liu, W., Jia, Y., Sermanet, P., Reed, S., Anguelov, D., Erhan, D., Vanhoucke, V., Rabinovich, A., 2015. Going deeper with convolutions. In: Proceedings of the IEEE Conference on Computer Vision and Pattern Recognition, pp. 1–9.

Zhang, X., Qiao, Y., Meng, F., Fan, C., Zhang, M., 2018. Identification of maize leaf diseases using improved deep convolutional neural networks. IEEE Access 6, 30370–30377.